Spatial Subsidies and Mortality of an Estuarine Copepod Revealed Using a Box Model

4 authors, including:

Anne Slaughter
San Francisco State University
10 PUBLICATIONS **190** CITATIONS

SEE PROFILE

John R. Durand
University of California, Davis
35 PUBLICATIONS **210** CITATIONS

SEE PROFILE

Some of the authors of this publication are also working on these related projects:

Integrating Surveys of the San Francisco Estuary View project

CrossMark

Spatial Subsidies and Mortality of an Estuarine Copepod Revealed Using a Box Model

Wim J. Kimmerer[1] · Edward S. Gross[2,3] · Anne M. Slaughter[1] · John R. Durand[3,4]

Abstract
Mortality of planktonic populations is difficult to determine because assumptions of the methods are rarely met, more so in estuaries where tidal exchange ensures violation of the assumption of a closed or spatially uniform population. Estuarine plankton populations undergo losses through movement from productive regions, creating a corresponding subsidy to regions that are less productive. We estimated mortality rates of the copepod *Pseudodiaptomus forbesi* in the San Francisco Estuary using a vertical-life-table approach with a Bayesian estimation method, combined with estimates of spatial subsidies and losses using a spatial box model with salinity-based boundaries. Data came from a long-term monitoring program and from three sample sets for 1991–2007 and 2010–2012. A hydrodynamic model coupled with a particle-tracking model supplied exchange rates between boxes and from each box to several sinks. In situ mortality, i.e., mortality corrected for movement, was highly variable. In situ mortality of adults was high (means by box and sampling program 0.1–0.9 day^{-1}) and appeared invariant with salinity or year. In situ mortality of nauplii and copepodites increased from fresh (~ 0) to brackish water (means 0.4–0.8 day^{-1}), probably because of consumption by clams and predatory copepods in brackish water. High mortality in the low-salinity box was offset by a subsidy which increased after 1993, indicating an increase in mortality. Our results emphasize the importance of mortality and spatial subsidies in structuring populations. Mortality estimates of estuarine plankton are feasible with sufficient sampling to overcome high variability, provided adjustments are made to account for movement.

Keywords *Pseudodiaptomus forbesi* · Population dynamics · Estuarine circulation · Gross Exchange Matrix · Bayesian analysis · San Francisco Estuary

Introduction

The dynamics of closed natural populations are a result of spatial and temporal patterns of birth, development, and mortality. In many aquatic organisms such as copepods, birth, and development are readily measured and are most strongly influenced by body size, temperature, and food availability (Hirst and Bunker 2003), as well as environmental stresses such as salinity or contaminants (Johnson 1980; Hook and Fisher 2001). By contrast, mortality is the most difficult population parameter to estimate (Ohman and Wood 1995; Ohman 2012).

Many factors may contribute to mortality including aging, poor nutrition, predation, disease, and parasitism. These factors can be strongly variable in space and time and are usually very difficult to estimate quantitatively. For example, fish that prey on zooplankton often occupy specific habitats such as shoals, or may school so that their predatory influence is patchy and episodic (Koslow 1981; Genin et al. 1988). In addition, most of the factors contributing to mortality can be estimated only indirectly, e.g., through gut content analysis of suspected predators. These methods may miss important components of mortality, such as consumption of early life stages by filter feeders (MacIsaac et al. 1991) and non-predatory mortality

✉ Wim J. Kimmerer
kimmerer@sfsu.edu

1 Estuary & Ocean Science Center, San Francisco State University, 3150 Paradise Dr., Tiburon, CA 94920-1205, USA

2 RMA, 1756 Picasso Avenue, Suite G, Davis, CA 95618, USA

3 Center for Watershed Sciences, University of California, Davis, One Shields Avenue, Davis, CA 95616, USA

4 Department of Wildlife, Fish and Conservation Biology, University of California, Davis, One Shields Avenue, Davis, CA 95616, USA

including disease and parasitism (Kimmerer and McKinnon 1990; Tang et al. 2006).

For organisms such as copepods that grow by stages, methods for mortality estimation have been developed that use count data together with known stage durations and simplifying assumptions about mortality patterns across stages (e.g., Mullin and Brooks 1970; Aksnes and Ohman 1996). Vertical-life-table methods are the most commonly applied because they are based on individual samples and do not require following cohorts through time (Kimmerer and McKinnon 1987; Aksnes and Ohman 1996; Gentleman et al. 2012). Key assumptions of these methods are that the proportions of each life stage are stable through time and that the population can be treated as closed (Aksnes and Ohman 1996; Gentleman et al. 2012). An additional assumption of constant mortality over a series of stages is usually necessary to account for variability inherent in count data and uncertainty in estimates of stage duration (Kimmerer 2015).

A synthesis of global patterns of mortality in epipelagic copepods used a combination of in situ measurements and a simple steady-state model of population dynamics in which mortality must balance reproduction and development (Hirst and Kiørboe 2002). This synthesis demonstrated a remarkable degree of consistency in mortality patterns varying only weakly with body size and strongly with temperature. Strictly speaking, mortality is more than a population process: it depends on the highly variable ecosystem process of predation and should therefore not be answerable to general rules like those that have been derived for growth rates (Miller et al. 1977). However, a population's capabilities for reproduction and development imply an "affordable" level of mortality (Dam and Tang 2001) in that mortality must balance reproduction and development over the long term in a closed population.

If that is so, why attempt to measure mortality at all? A large part of the interest in mortality estimation is to explore its spatial and temporal patterns and try to understand the principal sources of this variability. In estuaries, we are interested in how patterns of mortality arise from patterns in causative agents such as hypoxia (Tiselius et al. 2008), diversions of water (Drinkwater and Frank 1994), sporadic or patchy predatory events (Koslow 1981), species-specific predation (Eiane et al. 2002), outbreaks of parasites (Kimmerer and McKinnon 1990), or other causes resulting in non-predatory mortality (Tang et al. 2006). Although each of these can be studied as a separate process, only through estimation of mortality overall can these components of mortality be placed into context (e.g., Kimmerer and McKinnon 1990).

In estuaries, spatial gradients in properties such as salinity and concentrations of nutrients and organic matter imply movement through advection and tidal dispersion. This in turn implies spatial subsidies of these properties from regions of abundance to depleted regions (Odum 1980; Nixon et al.

1986; Polis et al. 1997). Likewise, spatial gradients in abundance of planktonic organisms together with estuarine transport processes can cause regions of positive net production to subsidize populations in unproductive regions.

The dynamics of a population that is actively exchanging between productive and unproductive regions therefore contains an additional term—the time rate of change of a local population depends on rates of birth, development, mortality, and movement to and from that population. This violates a key assumption of extant methods of estimating mortality, that of a closed or spatially uniform population. Therefore, to be able to estimate mortality and to understand the spatial distribution and important causes of mortality, movement must be taken explicitly into account.

Here, we estimate spatial subsidies and mortality of the introduced copepod *Pseudodiaptomus forbesi* in the San Francisco Estuary (SFE) as part of a broader investigation of population dynamics. Spatial gradients and strong tidal currents implied a subsidy of copepods into the low-salinity region of the estuary (Kayfetz and Kimmerer 2017) and precluded making the assumption of a closed or spatially uniform population. We therefore estimated movements of copepods using a simple spatial- and salinity-based box model based on three-dimensional hydrodynamic and particle-tracking models and then used this movement to adjust mortality estimates made by a modified vertical-life-table method (the "Constant" method of Kimmerer 2015). We refer to the mortality calculated from data on local population dynamics as "apparent mortality" and mortality corrected for movement as "in situ mortality" to highlight its dependence on local processes such as predation.

Methods

Overview

The study area was the upper San Francisco Estuary (SFE) including San Pablo and Suisun Bays and the California Delta, where the Sacramento and San Joaquin Rivers meet (Fig. 1). The climate of this region is Mediterranean, with wet winters–springs and dry summers–autumns. During 1980–2012, median annual inflow to the estuary was 752 m^3 s^{-1}, approximately three quarters of which occurred during December to June. A system of reservoirs and canals stores water during the wet season and releases it for agriculture and urban uses throughout the basin, with highest use during the dry season. Massive pumps in the southern Delta can divert up to 340 m^3 s^{-1}, much of which is exported from the basin. The calculated flow from the Delta into Suisun Bay (Fig. 1), essentially inflow less diversions and net consumption within the Delta, is called "net Delta outflow." Low precipitation coupled with water storage and diversions results in

Fig. 1 Maps of study area showing boundaries of spatial boxes (heavy lines) for hydrodynamic model runs under two flow scenarios. **a** 190 m^3 s^{-1}, X2 = 79 km, close to the median for all of the sample data. **b** 370 m^3 s^{-1}, X2 = 67 km. Symbols in **a**, locations of transect stations (sample set T, circles and squares; data from stations shown as larger squares not used, see text) and long-term monitoring stations (data set M, triangles; sample set R, open triangles). Stations for sample set S not shown as locations varied with salinity
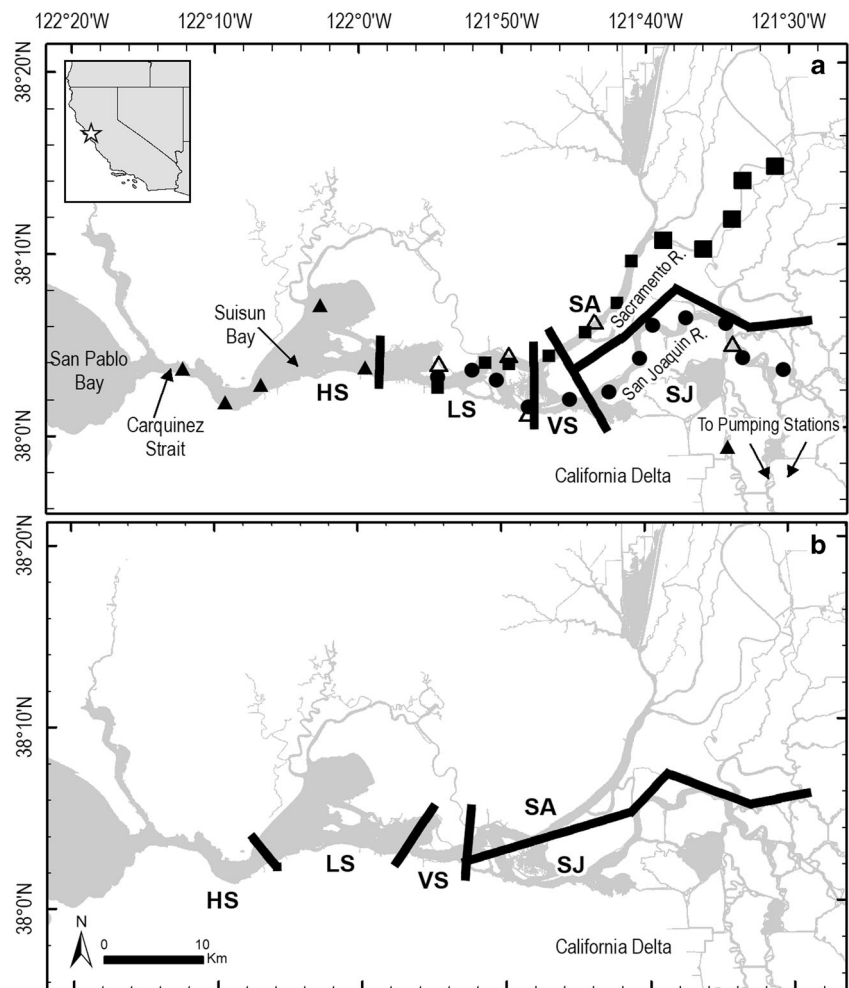
low flow during July–October in most years with a median net Delta outflow of 156 m^3 s^{-1}.

Pseudodiaptomus forbesi was first discovered in the SFE in 1987, became abundant in 1988 (Orsi and Walter 1991), and has since remained abundant in freshwater and moderately abundant in brackish waters of the estuary. A tropical to subtropical species, *P. forbesi* is abundant in the SFE only during summer–autumn. It is the principal summertime prey of the endangered delta smelt, *Hypomesus transpacificus* (Slater and Baxter 2014), and important in the diets of other fishes (Bryant and Arnold 2007). Low abundance of *P. forbesi* and other copepods in the low-salinity region of the estuary in recent years (Kayfetz and Kimmerer 2017) may have contributed to declines in abundance of delta smelt and other fish species (Sommer et al. 2007; Baxter et al. 2010; Kimmerer and Rose 2018). Although adult *P. forbesi* are generally considered demersal (Walter 1989), in the SFE they occur throughout the water column except where light penetrates to the bottom (Kimmerer and Slaughter 2016).

We combined abundance estimates of *P. forbesi* from a long-term monitoring program (data set M) with estimates of exchange among spatial boxes determined using a particle-tracking model. Three sets of samples were used to estimate mortality within each box (Table 1). These sample sets were collected at different times for different purposes and therefore differ in sampling intensity and in the life stages included. Sample set R (Recount) comprised a selection of archived samples from data set M that we recounted to obtain counts by copepodite stage and sex and for egg ratios. Samples were taken from a subset of stations in July and August (the period of maximum abundance of *P. forbesi*) during 1991–2007, although most samples before 1996 were too deteriorated to be usable. Sample set S (Salinity) was obtained from four stations determined by salinity, visited monthly during 2003–2004. Sample set T (Transect) was obtained through a series of transects across the habitat of *P. forbesi* during August–October of 2010–2012 (Kimmerer et al. 2017). Apparent mortality was estimated using raw count data from each sample set by a Bayesian fitting method (below).

We developed a box model comprising five spatial boxes whose junctions are defined dynamically by salinity, and three sinks. A particle-tracking model (PTM) used output from a three-dimensional hydrodynamic model to determine proportional movement from each box to each other box and to each

Table 1 Summary of samples in the historical monitoring data (data set M) used to estimate transport and in sample sets R, S, and T analyzed for mortality

Sample source	Data set M: Historical Monitoring data	Sample set		
		R Samples from long-term monitoring	S Stations by salinity	T Transects
Years	1990–2012	1991–2007	2003	2010–2012
Months	June–October	July–August	June–October	August–October
Stations	18 (Max)	8 (Max)	4 (Salinity)	12 (San Joaquin), 7 (Sac)
Total samples used	647	108	20	84
Net diameter (cm)	12.7	12.7	50	50
Net mesh (μm)	154	154	53	53
Type of tow	Oblique	Oblique	Vertical	Vertical
Counts:				
Eggs	–	422 (0–3968)	Not used	427 (28–1434)
Nauplii	Used only for Fig. 3	Not counted	Staged 138 (47–554)	Counted 181 (2–1211)
Copepodites	Not staged	672 (47–2187)	86 (9–699)	581 (52–11,339)
Adults	Not sexed	Sexed 534 (49–2826)	Sexed 344 (5–1256)	Sexed 322 (60–856)
Mortality methods:				
Nauplii		Eqs. A3–A5	Standard	Eqs. A3–A6
Copepodites		Eq. A1	Standard	Standard
Adults		By sex	By sex	By sex

The number of samples is the total analyzed for distribution patterns (monitoring data) or mortality (sample sets R, S, and T). Numbers in parentheses are ranges of individual counts per sample. Mortality calculations described as "standard" or "by sex" used methods in Kimmerer (2015)
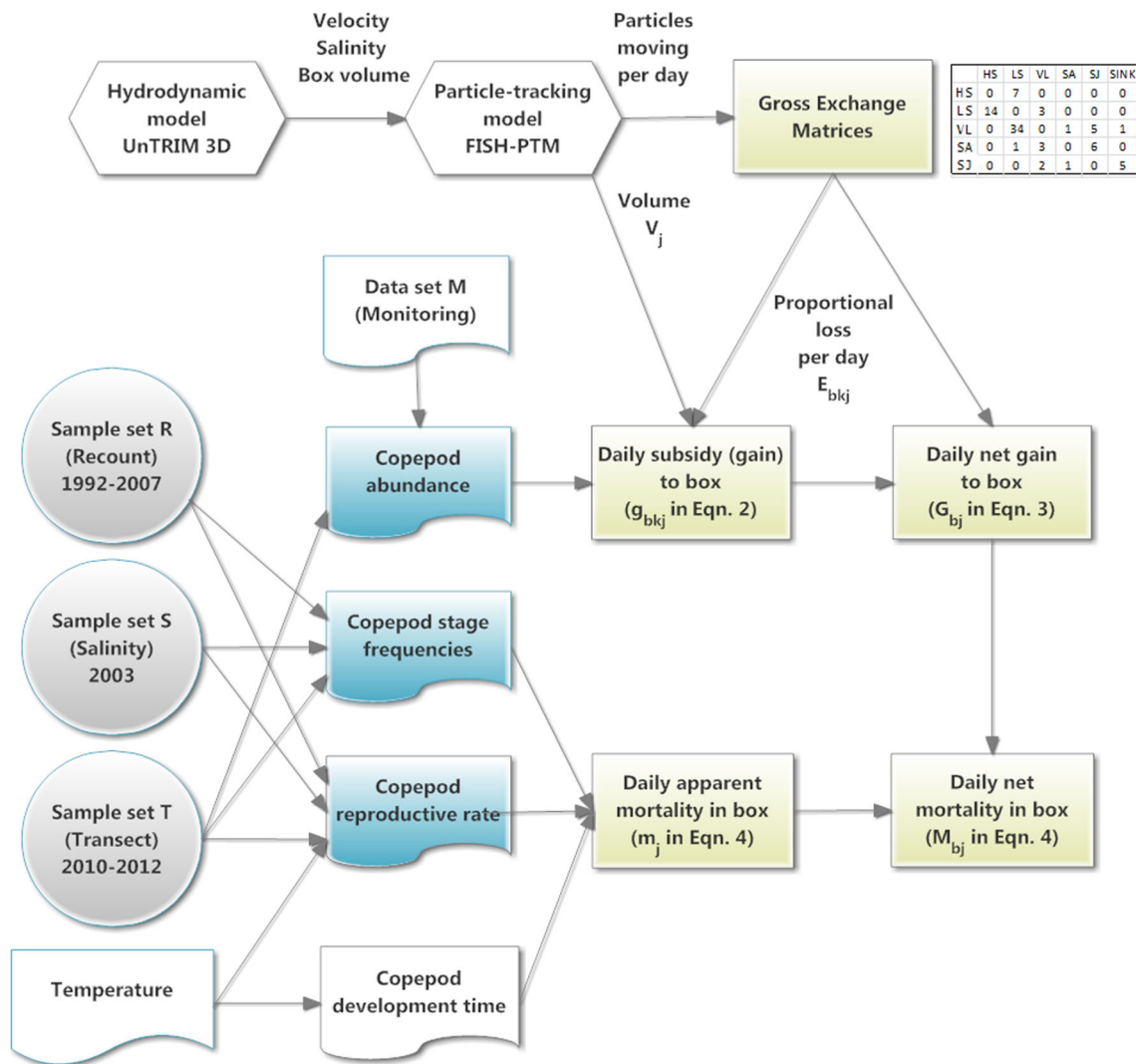
sink. Abundance data were used to convert proportional movement from source boxes into proportional gains (i.e., subsidies) to populations in recipient boxes. The proportional losses and gains were then used to analyze patterns of subsidy and to determine in situ mortality from apparent mortality and spatial losses and gains. A flow diagram (Fig. 2) may help readers to follow the analytical process.

Box Model

The three-dimensional UnTRIM San Francisco Bay–Delta Model (MacWilliams and Gross 2013; MacWilliams et al. 2015) was used to simulate hydrodynamic conditions. The spatial scope of this model extends from the Pacific Ocean through the entire estuary. Instantaneous values of water level, velocity, and eddy diffusivity were archived to files every half hour as input to the PTM. Because of the long time period to be modeled, it was impracticable to model the entire time series, and because our study focused on the dry season, the variability in flow was small. Therefore, we used output from model runs with four steady freshwater flows, and results (below) were interpolated between these values. In addition, tidal periods were adjusted to 12 and 24 h to eliminate spring-neap variability. These and higher flows and all other boundary conditions had been established, and model runs performed, for use in a previous analysis of habitat for fish (Kimmerer et al. 2013).

The Flexible Integration of Staggered-grid Hydrodynamics Particle Tracking Model (FISH-PTM; Gross et al. 2010) estimates particle trajectories in three dimensions using velocities and eddy diffusivity calculated by UnTRIM. The backward Itô stochastic differential equation (LaBolle et al. 2000) was used to estimate diffusive transport of particles. Advective transport used node velocities estimated from normal velocities provided by UnTRIM at cell faces using the nRT2 method described by Wang et al. (2011). Then, velocity was interpolated from node velocity values by the method of generalized barycentric coordinates (Meyer et al. 2002). The time step for both advection and diffusion was adjusted such that displacements in a time step do not exceed vertical or horizontal cell spacing. A previous study used results from FISH-PTM to assess the ability of estuarine organisms including *P. forbesi* to remain within regions of the estuary through tidal vertical migration (Kimmerer et al. 2014).

The five spatial boxes spanned the habitat of *P. forbesi* (Fig. 1). The extent of each box was determined partly by geography and partly by salinity to resolve broad patterns in the observed distribution of *P. forbesi*. The easternmost boxes include the Sacramento River box (SA) which includes the northern California Delta and extends into Suisun Bay to include all waters outside the southern and central Delta at salinity < 0.2, and the San Joaquin River box (SJ) which always covers the southern and eastern Delta (neglecting high salinity coming from agricultural drainage), and includes central Delta waters at salinity < 0.2. The boundaries between these boxes

The table in the figure (Gross Exchange Matrix example):

	HS	LS	VL	SA	SJ	SINK
HS	0	7	0	0	0	0
LS	14	0	3	0	0	0
VL	0	34	0	1	5	1
SA	0	1	3	0	6	0
SJ	0	0	2	1	0	5

Fig. 2 Flow diagram of calculations; shaded shapes represent calculations made for this paper, while other calculations are by reference. Hexagons are three-dimensional simulation models; circles are sample sets; document shapes are data sets, either external or derived from sample sets; rectangles are results of calculations based on data and 3-D model output. Temperature was from field samples. The table in the upper right is one example of a Gross Exchange Matrix

and their landward extents were fixed. The three remaining boxes were defined by salinity to include a very low-salinity box (VL, salinity 0.2–0.5), a low-salinity box (LS, 0.5–5.0), and a high-salinity box (HS, above 5.0) (Fig. 1). The low-salinity box was the principal focus of the study because of high and variable mortality there and because of its importance as habitat for delta smelt. The high-salinity box had an open seaward boundary, and mortality was not calculated for this box. We refer to the other four boxes together as the model domain.

The three sinks were points in the model where particles were permanently lost from the simulation. Particles could be entrained in large pumping plants that divert water from the southern Delta (Fig. 1) or in any of the numerous smaller diversions throughout the Delta (MacWilliams et al. 2015). A negligible fraction of particles was also trapped in drying cells during falling tide (median 0.02%, maximum of 0.2% of particles).

Transport processes were represented by daily mixing between boxes using the "Gross Exchange Matrix" approach (Kremer et al. 2010). Each box was seeded with a spatially uniform density of particles (1 particle per 5000 m^3 or ~ 250,000 total particles), and after 24 h of movement in the particle-tracking model, the distributions of particles that originated in each source box were analyzed. The fraction of particles released in each box and then recovered in each box and sink was calculated and placed in the Gross Exchange Matrix. The volume of water in each box was also determined for calculations of proportional movement.

Eight Gross Exchange Matrices were determined, one for each of the four steady flows and for two particle behaviors. These were passive (neutrally buoyant) behavior, and tidal

migration with upward swimming at 0.25 mm s^{-1} during flood and downward swimming at 0.75 mm s^{-1} during ebb. This tidal migration behavior resulted in the closest match of vertical distributions of particles to distributions of adult copepods and copepodites in the estuary and allowed for retention in the estuary except at the highest flow (Kimmerer et al. 2014).

Copepod Data

Locations for all three sample sets were determined with GPS; salinity and temperature were measured with a SeaBird SBE-19 CTD or a YSI Model 30 sonde. Samples were collected by plankton net tows in deep parts of the channels (Table 1; Fig. 1) and preserved with 4% formaldehyde and Rose Bengal stain. Subsamples for mortality estimates were taken by piston pipette and copepodites were identified to stage and copepodite stage 5 and adults to sex; differences among analyses used for sample sets are described below and in Table 1.

Data Set M: Historical Monitoring Data Since 1972, the Interagency Ecological Program has collected zooplankton samples monthly or twice monthly throughout the northern estuary (Orsi and Mecum 1986; metadata at http://www.water.ca.gov/bdma/meta/zooplankton.cfm). For this study, we used reported abundance of *P. forbesi* adults (not sexed) and *Pseudodiaptomus* spp. copepodites (not staged) from 1990 to 2012. Additional samples taken with a pump for organisms smaller than 154 μm were analyzed for nauplii, but *P. forbesi* nauplii were identified only from 2000 on, and in very small subsamples until 2008, so these data were not used except to explore broad patterns of abundance in salinity space. Surface salinity was determined from reported electrical conductance (Practical Salinity Scale, UNESCO 1981). Patterns of abundance of each life stage in salinity space were determined by dividing the salinity range into 25 bins of equal number of data values, then calculating the median abundance for each life stage in each bin. This was done for July–October 1995–2012 (2000–2012 for nauplii), because a shift in spatial distribution of *P. forbesi* had occurred around 1993 (Kayfetz and Kimmerer 2017).

Sample Set R (Recount) Data for mortality estimates were obtained by recounting archived net samples from the monitoring program (data set M) which were available for August of 1991 and July–August of 1992 and 1994–2007. Nauplii were not counted. Stations were selected to extend across the salinity gradient (Fig. 1). One station (NZM10, not shown) was eliminated from the analysis because catches contained relatively few adult females, which presumably are on the bottom by day at this clear, shallow location (Kimmerer and Slaughter 2016).

Sample Set S (Salinity) We sampled zooplankton in the upper SFE (Fig. 1) from March 2003 through March 2004 and for this analysis used samples from June to October 2003 (see Durand 2010). Four salinity-based stations were chosen in main channels at surface salinity 2 and 0.5 in Suisun Bay, at 0.1 in the Sacramento River, and at 0.1 in the San Joaquin River. Counts of stage 5 copepodites by sex were low in about half of the samples, so mortality of adults was calculated for both sexes combined.

Sample Set T (Transect) During August–October 2010–2012, we conducted a total of five transects up the Sacramento River and five up the San Joaquin River to sample for zooplankton (Kimmerer et al. 2017; Fig. 1). On each transect, 12 stations were established at 3-km intervals. The five easternmost stations on the Sacramento River (Fig. 1) were omitted from further analysis because calanoid copepods including *P. forbesi* were consistently uncommon in this more riverine and less tidal region of the estuary. Nauplii were counted but not staged.

Calculating Apparent Mortality

Mortality of nauplii, copepodites, and adults was calculated for each sample using various modifications (see Supplementary Information) of the Bayesian method described by Kimmerer (2015). This method gives mortality estimates by major life stage under the assumptions that the population age structure is not changing too rapidly and that immigration and emigration are in balance. The former assumption is unlikely to be met in this dynamic environment, but errors introduced by violations should be averaged out over many samples. The imbalance of immigration and emigration is often large, requiring the correction for movement (below). Bayesian analyses were conducted in WinBUGS version 1.4.3 and other analyses in R version 3.2.3 (R Development Core Team 2015).

Information on calculation of mortality for populations that do not form cohorts is available from several sources (Aksnes and Ohman 1996; Hirst and Kiørboe 2002; Gentleman et al. 2012). We applied the Constant model originally used by Kimmerer and McKinnon (1987) and described in detail by Kimmerer (2015). Inputs to the analysis consisted of stage durations of eggs, nauplii, and copepodites, and counts of stages that varied among sample sets (Table 1). The duration of the egg stage was calculated from temperature at the time of sampling (Sullivan and Kimmerer 2013). Stage durations of nauplii and copepodites were determined in laboratory experiments at 22 °C with saturating food (Kimmerer et al. 2017) and adjusted for temperature at the sampling station using the relationship of egg duration to temperature. An additional adjustment for the effects of food limitation was incorporated, based on results from molt-rate experiments

performed during the 2010–2012 study, and used in the analysis of sample set T (Kimmerer et al. 2017). Because those results were only weakly related to chlorophyll concentration, for sample sets R and S, we used the means and standard deviations of Φ, the ratio of laboratory to field development times from the molt-rate experiments, which were 0.50 ± 0.16 for copepodites and 0.29 ± 0.20 for nauplii (Kimmerer et al. 2017). Samples from these distributions were truncated to be > 0 in the Bayesian analysis.

Applying the Box Model to the Copepod Population

The box model was applied under the assumption that the subsidies due to transport to each box would be balanced by losses due to transport from and birth and mortality within the box. The Gross Exchange Matrices from the particle-tracking model were used to estimate the movement of copepods of each major life stage (nauplii, copepodites, adults) between boxes. Copepodites and adults were assumed to migrate tidally (Kimmerer et al. 2002, 2014), and nauplii were assumed to move as passive particles (Schmitt et al. 2011).

Movements were expressed as losses from one box and subsidies to another box as proportions of abundance within that box, for a given freshwater flow; the development below applies to a single flow value to simplify terminology. The proportional losses from each box are elements of the Gross Exchange Matrices and are independent of abundance:

$$E_{bjk} = \frac{P_{bk,t=1}}{P_{bj,t=0}} \qquad (1)$$

where E_{bjk} is the element of the Gross Exchange Matrix giving proportional losses of copepods from box j to box k for vertical behavior b, which is either tidal vertical migration for copepodites and adults or passive for nauplii. $P_{bj,t=0}$ is the number of particles released in box j at the beginning of the PTM run, and $P_{bk,t=1}$ is the number of those particles that are in box k (or sink k) after a 1-day PTM run.

Proportional subsidies to each box depend on differences in abundance between pairs of boxes:

$$g_{bkj} = \frac{n_k E_{bkj} V_k}{n_j V_j} \qquad (2)$$

Here, g_{bkj} is the subsidy or proportional gain in numbers of a particular major life stage due to movement from box k into box j (note order of subscripts is switched to reflect movement into box j), n_j and n_k (m^{-3}) the mean copepod abundance, and V_j and V_k (m^3) the box volume, in boxes j and k, respectively. Then net gain G_{bj} into box j is the sum of proportional

subsidies from each other box minus the sum of losses from box j to each other box and sink:

$$G_{bj} = \sum_{k \neq j} g_{bkj} - \sum_{k \neq j} E_{bjk} \qquad (3)$$

and apparent mortality m_j in box j is corrected for gains and losses through movement to give in situ mortality M_{bj} in box j for behavior b:

$$M_{bj} = m_j + G_{bj} \qquad (4)$$

Particle-tracking model output included the Gross Exchange Matrix E and the volume V of each box for each of the four steady flows. To determine values of E corresponding to each sampling date, we interpolated each matrix element using X2, the distance up the axis of the estuary to a near-bottom tidally averaged salinity of 2 (Jassby et al. 1995; MacWilliams et al. 2015), a value roughly in the center of the low-salinity box. X2 incorporates the ~ 2-week lag time in the response of salinity to flow, and the along-axis salinity distribution in the San Francisco Estuary is approximately self-similar (Monismith et al. 2002); therefore, a given X2 implies the spatial distribution of all of the salinity-based boxes. X2 values for each day of the historical record were calculated (Jassby et al. 1995), and those for each flow in the matrix E were determined from the hydrodynamic model. Then, each day's value of E was interpolated linearly in the X2 values. The four steady flows were 100, 190, 370, and 730 m^3 s^{-1}, corresponding to X2 values of 90, 79, 67, and 58 km, respectively.

From Eq. 4 it is clear that the net gain G_{bj} is a key component in the calculation of in situ mortality, and therefore it is correlated with in situ mortality. Since net gain G_{bj} was available for all years, we examined the time course and relationship of net gain to X2 for copepodites and adults as a surrogate for in situ mortality. Abundance was calculated from the long-term monitoring program. Year was modeled as a step function with a single breakpoint between 1993 and 1994 to correspond with the expected effects of the introduction of the predatory copepod *Acartiella sinensis* (Slaughter et al. 2016).

Abundance values for Eq. 2 were determined separately for each box and somewhat differently for each sample set. For sample set R, data from July and August of each year were obtained from long-term monitoring (data set M, $N = 23$–43 depending on year; Table 1). For sample set S, we used monitoring data for June–October 2003 ($N = 69$; Table 1). In both cases, we used geometric means of data in the Sacramento and San Joaquin boxes. Sampling was sometimes spotty in the salinity-based boxes, so their abundance values were determined by smoothing. For each year, the log of abundance was first modeled as a function of the log of salinity using a generalized additive model with a spline-based smoother (function *gam* in R with $k = 5$). Predicted values were then

averaged across the range of salinities in each salinity-based box.

Counts of nauplii in data set M were too low to estimate the subsidy g_{bkj} in Eq. 2. We assumed a correspondence of spatial gradients in abundance of nauplii with those of copepodites, since their patterns among spatial boxes were similar (see "Results"). Then we substituted copepodite abundance for that of nauplii in Eq. 2, with vertical behavior b set for passive particles to represent the limited swimming ability of nauplii (Schmitt et al. 2011).

Data for abundance by box from sample set T were averaged within each box based on location and salinity. The maximum salinity on the transects was 4, so no data were obtained from the high-salinity box; abundance in that box was assumed to be negligible, so dispersion of copepods from this box to the low-salinity box was assumed to be negligible for sample set T only.

Results

Historical Patterns

Historical monitoring (data set M) showed persistent patterns in summer–autumn by which abundance of *Pseudodiaptomus forbesi* was highest in freshwater and declined with increasing salinity (Fig. 3). The regions of high abundance shifted ontogenetically: abundance of nauplii during 2000–2012 was at least 25% of its maximum (gray horizontal line in Fig. 3) at salinity between 0.07 (the median of the lowest-salinity bin) and 0.42, while the same values for copepodites during 1994–2012 were 0.07 and 0.56, and those for adults were 0.07 and 2.81. Abundances of nauplii and copepodites were closely correlated in sample sets S ($r = 0.92$, $N = 26$) and T ($r = 0.72$, $N = 139$), supporting the use of the annual spatial patterns of copepodites to approximate those of nauplii for calculating movement using data set M.

Freshwater flow into the estuary is least variable during summer–autumn. Nevertheless, variation in summer freshwater flow into the estuary resulted in interannual swings of ∼ 30 km in the position of the salinity field as indexed by X2, notable by the low values during the two wettest years, 1995 and 1998 (Fig. 4a). Interannual variation in summer flow had little effect on copepod abundance (Fig. 4b–e), which was generally lower to the west than the east, and declined during 1990–1994 particularly for adults in the low-salinity and Sacramento boxes. Copepodites in the low-salinity box were more abundant than adults during 1995 and 1998 but averaged ∼half as abundant in other years (Fig. 4b). In the San Joaquin box (Fig. 4e), copepodites were approximately twice as abundant as adults on average, and these stages were about equally abundant in the remaining boxes (Fig. 4c, d).
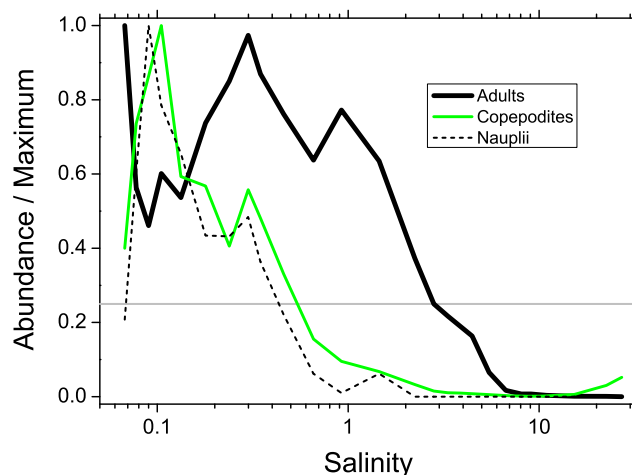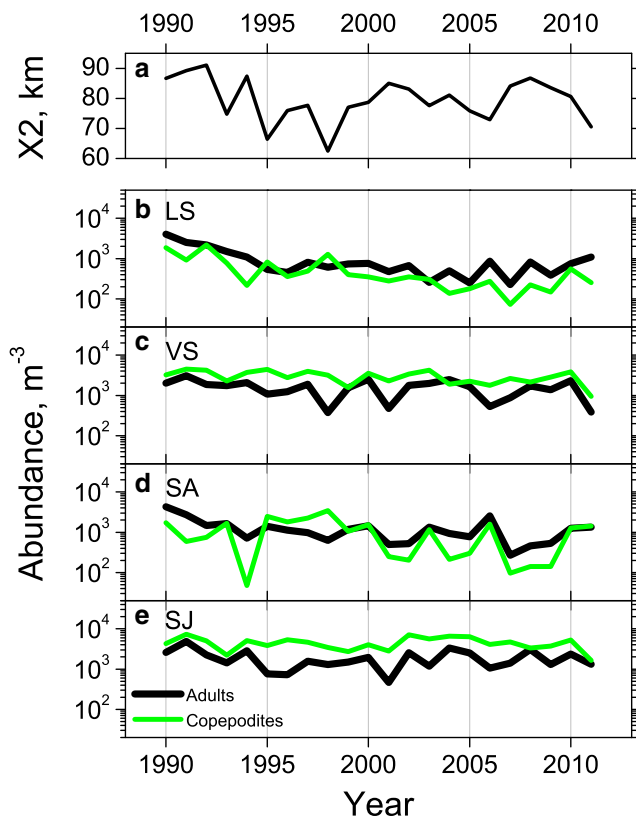

Fig. 3 Abundance of *Pseudodiaptomus* spp. copepodites and nauplii (not identified to species) and *P. forbesi* adults as functions of surface salinity, scaled to the maximum for each life stage. Data from data set M for each life stage were assigned to 25 salinity bins of equal numbers of data points to eliminate bias due to the greater sampling effort at low salinity; then, medians of each bin were divided by the maximum for that life stage. Salinity axis is log-transformed to focus on low salinity. The increase in relative abundance of copepodites at salinity > 10 probably reflects the contribution of *P. marinus*. The gray horizontal line indicates a median abundance of 25% of the maximum

Subsidies and Losses

Smoothed abundance data for each year in the long-term data were used to calculate representative values of abundance for the salinity-based boxes. Examples of 4 years of data for copepodites (Fig. 5) show the smoothers fit the data reasonably well, including the data from both data set M and sample set S for 2003 (Fig. 5c). In 1991 (Fig. 5a), the smoothed line was nearly linear (with both variables shown on a log scale). Patterns after 1993 generally showed a downward inflection of the curve at salinity of ∼ 0.5 (Fig. 5c). An exception occurred in 1998, the highest-flow year, when the inflection shifted to salinity ∼ 1 (Fig. 5b); other high-flow years (Fig. 4a) had similar shifts in inflections. The year 2007 had an unusually steep inflection and low abundance at salinity > ∼ 1 (Fig. 5d). Patterns for adults (not shown) were generally flatter with the downward inflection point usually occurring at a higher salinity than that for copepodites, as suggested for aggregated data in Fig. 3.

Losses and subsidies of copepods (Fig. 6; example in Table 2) varied spatially, and subsidies also varied by life stage because of behavioral differences and because subsidies depended on spatial gradients (Eq. 2). Total losses of copepods from each of the four spatial boxes to boxes further seaward (i.e., from each box to all boxes further west) generally increased with decreasing X2 (increasing freshwater flow; Fig. 6a–h), presumably because of an increasing contribution of advection to transport. Landward losses, including losses to the three sinks, were generally less affected than seaward
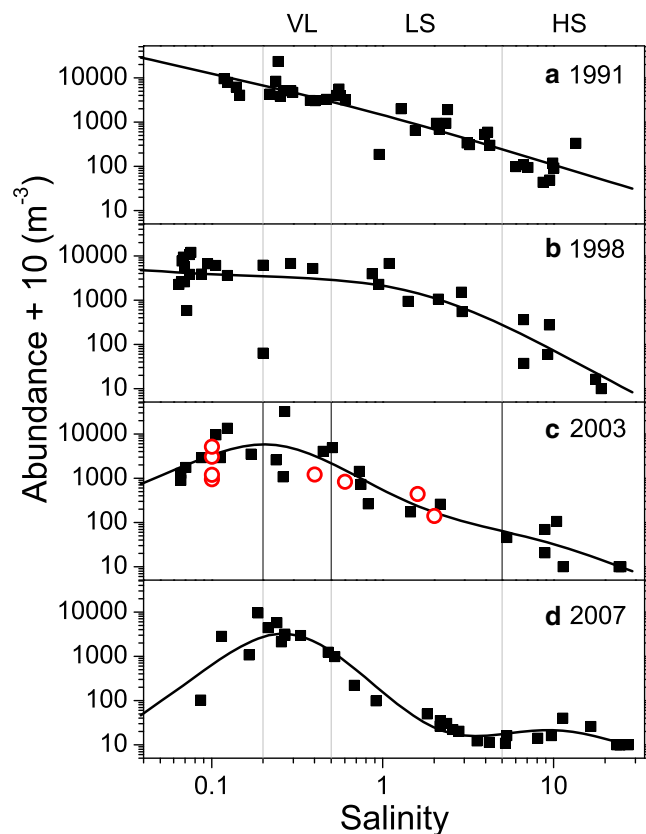
Fig. 4 Mean flow conditions and abundance of *Pseudodiaptomus forbesi* by year for July–August. **a** X2, the distance up the axis of the estuary to a salinity of 2, an index of the physical response of the estuary to freshwater flow. **b**–**e** Mean abundance of copepodites and adults for model boxes: **b**, low-salinity; **c**, very low-salinity; **d**, Sacramento River; **e**, San Joaquin River

Fig. 5 Examples illustrating use of GAMs to estimate abundance of *P. forbesi* copepodites by salinity box. Abundance values have been increased by 10 to allow for zeros. Labels at top and vertical lines indicate boundaries of salinity-based boxes. Filled squares, sample set R; open circles, sample set S from 2003 only. **a** 1991 before the spatial shift in *P. forbesi* in 1993–1994. **b** 1998, the highest-flow year (Fig. 4a) when the entire population was shifted toward higher salinity. **c** 2003 which was similar to all other years after 1998 except 2007. **d** 2007 when abundance at salinity > 1 was exceptionally low

losses both by freshwater flow and by particle behavior (Fig. 6a–h). Freshwater flow had a substantial effect on landward losses only in the San Joaquin River box (Fig. 6d, h), because as the spatial extent of this box shrank with movement of the salinity field further into the estuary, the proportional loss of particles to water diversions in the Delta increased. Tidally migrating particles were lost to seaward at a lower rate and to landward at a higher rate than passive particles in the very low- and low-salinity boxes (Fig. 6a, b, e, f), where salinity stratification can occur in the deeper channels, making tidal vertical migration highly effective for retention. Particle behavior had a negligible effect in the two freshwater river boxes (Fig. 6c, d, g, h).

Total subsidies of copepods to each box as a proportion of abundance within the box ($\sum\limits_{k \neq j} g_{bkj}$ in Eqs. 2 and 3) differed among boxes and life stages (Fig. 6i–l). High variability in sample data also propagated into estimates of the subsidies. Proportional subsidies of nauplii in sample set T were higher than total losses in the low- and very low-salinity boxes (Fig. 6a, b, e, f, i, j) owing to steep abundance gradients (Fig. 3), but subsidies of nauplii to the two river boxes were low. Proportional subsidies of

nauplii to the low-salinity box were lower in 2012 than in other years but still exceeded losses at the low-flow conditions existing that year. The subsidies of nauplii to the San Joaquin box (Fig. 6l) were < 0.02 day^{-1}, consistent with high abundance in that box and low landward losses for passive particles in the low- and very low-salinity boxes (Fig. 6a, b, e, f).

Subsidies of copepodites to the low-salinity box were also higher (Fig. 6i) than losses (Fig. 6a), while subsidies of copepodites to the San Joaquin River box (Fig. 6l) were lower than losses (Fig. 6d). Subsidies of adults were roughly similar to losses for all but the Sacramento River box (Fig. 6k), where subsidies were low and mediated primarily by exchange with the San Joaquin box (not shown).

Net gains (i.e., subsidies–losses due to movement only; Eq. 3) were high for nauplii and copepodites into the low-salinity box, variable into the very low-salinity box, and between − 0.08 and 0.05 day^{-1} elsewhere. Net gains were low for adults
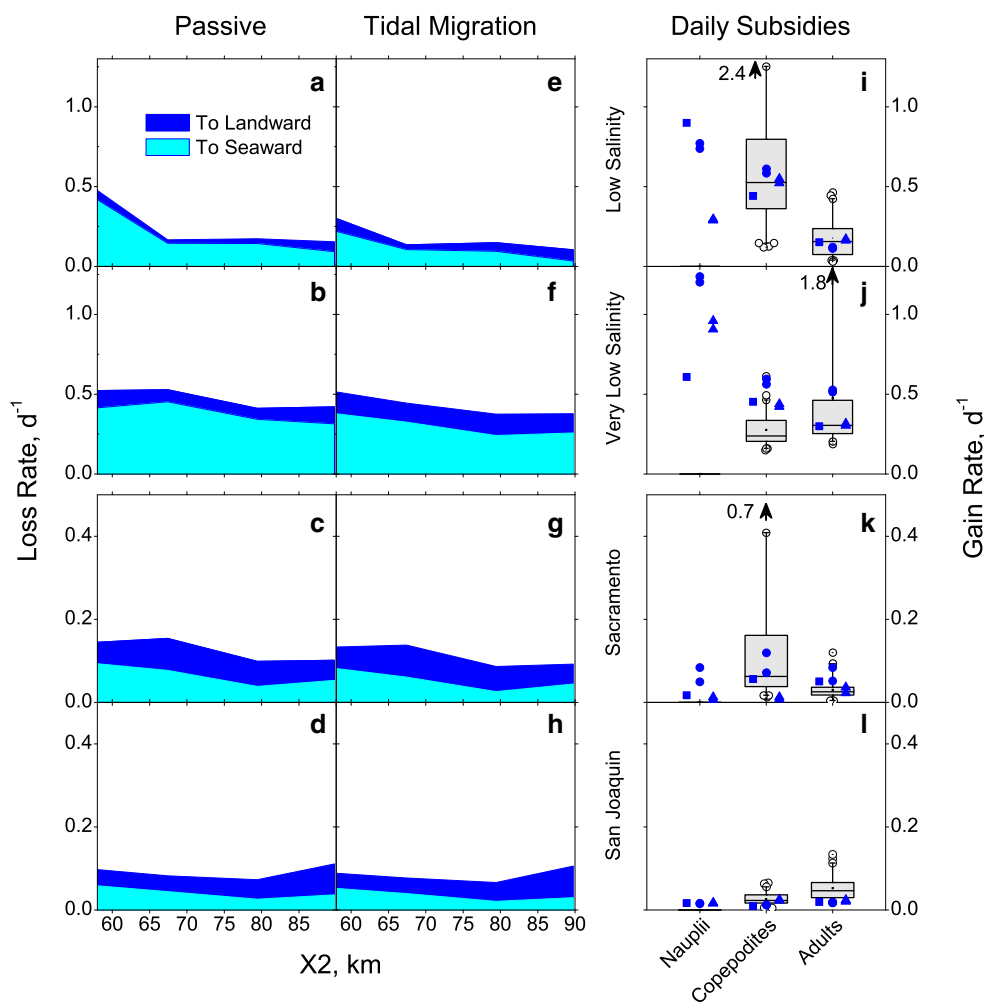
Fig. 6 Total losses of copepods from, and subsidies to, each spatial box as proportions of abundance in that box. **a–h** Losses based on Gross Exchange Matrices ($\sum_{k \neq j} E_{bjk}$ in Eq. 3) and separated into landward (dark band, where SJ is the most landward box and the three sinks are considered landward of all boxes) and seaward (light band) directions. **a–d** Cumulative area plots showing losses as a function of X2 (km) for passive particles. **e–h** As for **a–d** for particles undergoing tidal migration. **i–l** Boxplots showing total subsidies ($\sum_{k \neq j} g_{bkj}$ in Eq. 3) into box j from all

other boxes k for each life stage from sample set R; quartiles (horizontal lines), 5th and 95th percentiles (whiskers), and outliers (open circles). Arrows indicate values of additional outliers. Filled symbols indicate subsidies based on sample set T including nauplii; squares indicate 2010, circles 2011, triangles 2012; symbols are offset to separate them. Note differences in *y* axis scales between the top two and bottom two rows of panels

in all boxes (Table 3). This difference was due to the steeper gradients in abundance in earlier developmental stages than in adults (Fig. 3) and lower probabilities of movement in the two river boxes (Fig. 6).

Net gains of adults into the low-salinity box increased slightly after 1993 but the effect was small and confidence limits included zero (linear regression, step change = 0.11 ± 0.12 day^{-1}). Net gains of copepodites in the low-salinity box were positively related to X2 and showed a step increase between 1993 and 1994 (Fig. 7). Data from 1990 to 1993 were insufficient to determine whether the slope with X2 increased also between 1993 and 1994 (Fig. 7 inset). Presumably, net

gains of nauplii increased by a similar amount given the correlations between abundances of nauplii and copepodites (above).

Nauplii and copepodites in the low-salinity box were being subsidized from the landward boxes as a result of steep abundance gradients and, at times, high freshwater flow. However, some of the variability in these data illustrate the problems with the coarse spatial resolution and small sample size: a single high value of copepodite abundance in the Sacramento River produced an anomalously high subsidy to the low-salinity box (> 2 day^{-1}, Fig. 6i), which was excluded from subsequent calculations summarized in Table 3.

Table 2 Example of percentage subsidies and losses between pairs of model boxes and from boxes to sinks

	HS	LS	VL	SA	SJ	Sinks
Losses from box						
		To box or sink				
HS	0	7	0	0	0	0
LS	14	0	3	~0	0	~0
VL	0	34	0	1	5	1
SA	0	1	3	0	6	~0
SJ	0	~0	2	1	0	5
Subsidies from box	To box					
HS	0	1	0	0	0	
LS	128	0	1	0	0	
VL	0	101	0	1	~0	
SA	0	3	4	0	1	
SJ	0	3	22	6	0	
	Net gains to box					
	121	91	− 14	− 3	− 6	

Loss values are in relation to the source boxes and are elements of the Gross Exchange Matrix, E_{bjk} from Eq. 1. Subsidies are in relation to the receiving boxes, g_{bkj} from Eq. 2, and net gains to each box are G_{bj} from Eq. 3. Values shown as ~0 are non-zero values < 0.5%, while values shown as 0 are true zeros. Example is for passive particles using abundance data on copepodites from data set M for July 2012 with outflow = 190 m³ day⁻¹ and X2 ~ 80 km, the median of all data (Fig. 1a)
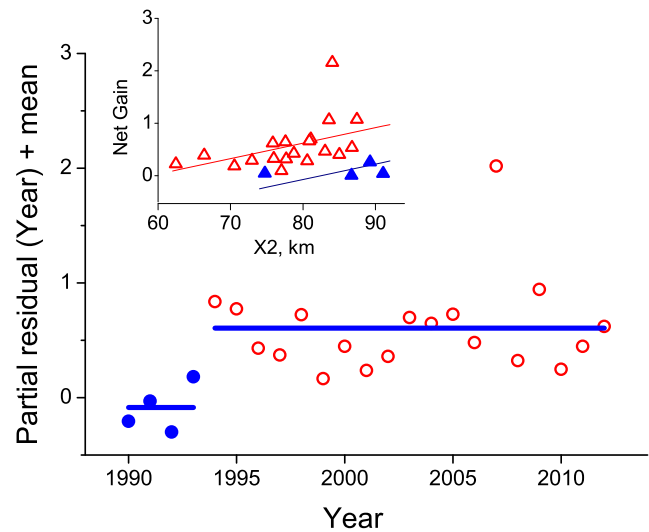
Mortality

Apparent mortality varied among life stages, spatial boxes, and sample sets (Table A2). Because many values had credible intervals that included zero, we focus on a handful of prominent patterns across the three sample sets. Apparent

Fig. 7 Net gains (Eq. 3) of *Pseudodiaptomus forbesi* copepodites into the low-salinity box by year; filled symbols, 1990–1993; open symbols, 1994–2012. Data are partial residuals plus grand mean from a linear regression of net gain on X2 and a step change between 1993 and 1994. The model is net gain = − 2.4 + (0.029 ± 0.026) X2 + (0.69 ± 0.49) f(year). Inset, net gains plotted against X2 with fitted lines from the regression model; filled symbols, 1990–1993, open symbols 1994–2012

mortality of nauplii was generally low in all boxes with a tendency to be positive in the low-salinity box and negative in the river boxes. Apparent mortality of copepodites was low to negative in the low-salinity box and slightly positive in the river boxes. Negative values of apparent mortality for nauplii and copepodites were at least partially a consequence of movement between boxes. Apparent mortality of adults was higher in the river boxes than in the low-salinity box and in most cases lower for males than for females. Two extreme

Table 3 In situ mortality, means with 95% confidence intervals by spatial box and life stage for each sample set

Stage	Sample set	Spatial box			
		LS	VL	SA	SJ
Nauplii (E)	R. Recounted from monitoring program (1991–2007)	**0.57 ± 0.09**	− 0.02 ± 0.19	− 0.01 ± 0.26	**− 0.11 ± 0.07**
Copepodites		**0.49 ± 0.10**	− 0.04 ± 0.08	**0.13 ± 0.12**	**0.11 ± 0.05**
Males		**0.21 ± 0.06**	0.08 ± 0.11	**0.21 ± 0.20**	**0.24 ± 0.07**
Females		**0.37 ± 0.06**	**0.27 ± 0.14**	**0.46 ± 0.33**	**0.38 ± 0.13**
Nauplii	S. Salinity-based (2003)	**0.80 ± 0.18**	0.04 ± 0.08	0.12 ± 0.30	0.05 ± 0.13
Copepodites		**0.41 ± 0.14**	**− 0.19 ± 0.18**	0.11 ± 0.12	0.04 ± 0.16
Adults		0.10 ± 0.09	0.06 ± 0.09	0.28 ± 0.35	**0.94 ± 0.85**
Nauplii (E)	T. Transect (2010–2012)	**0.56 ± 0.13**	**0.56 ± 0.16**	**− 0.16 ± 0.07**	**− 0.14 ± 0.02**
Nauplii (C)		**0.49 ± 0.11**	**0.43 ± 0.19**	**− 0.10 ± 0.08**	**− 0.17 ± 0.05**
Copepodites		**0.39 ± 0.06**	**0.23 ± 0.07**	**0.09 ± 0.07**	**0.13 ± 0.03**
Males		**0.10 ± 0.03**	0.16 ± 0.13	**0.18 ± 0.06**	**0.05 ± 0.04**
Females		**0.20 ± 0.06**	**0.20 ± 0.11**	**0.46 ± 0.19**	**0.19 ± 0.10**

Bold entries indicate estimates with confidence limits that do not include zero. Mortality of nauplii from counts (C) was calculated using Eq. A6 and that from egg production (E) using Eq. A4. Two samples with anomalously high net gains for copepodites in sample set R (see Fig. 6i) were eliminated from this analysis

values (both ~2 day^{-1}) in sample set S in the San Joaquin box raised the mean and expanded the confidence interval.

The two methods of estimating apparent mortality of nauplii in sample set T (Supplementary Information Eqs. A4–A6) gave similar results to each other across the spatial boxes, with rather large confidence intervals that overlapped between the two methods (Table A2). The estimates from the two methods were related by a geometric mean regression, m_n (Count method) = 0.025 + (0.75 ± 0.21) m_n (Egg method) (bootstrap confidence limits, $r = 0.57$, $N = 84$). Since the count method used more data (i.e., abundance of nauplii), it is probably more accurate than the egg method, implying that the apparent mortality of nauplii in sample set R determined by the egg method was slightly overestimated.

In situ mortality (Eq. 3) was highly variable among samples in the same box (Fig. 8; Table 3), but several consistent patterns emerged. All three sample sets showed an increasing trend in in situ mortality of nauplii and copepodites with increasing salinity, with the highest in situ mortality in the low-salinity box (Fig. 8a, b, e, f). In situ mortality of nauplii had negative means in the river boxes in sample sets R and T but positive in sample set S (Table 3; Fig. 8a, e), which was the only sample set in which naupliar mortality was determined from abundance by stage. In situ mortality of copepodites was similarly high in the low-salinity box and low but with positive means in the river boxes in all three sample sets. In situ mortality of copepodites from sample set S was negative in the very low-salinity box (Fig. 8b, f). In situ mortality of adults was moderate and roughly similar among boxes, with higher values for females than males and no strong pattern with salinity (Fig. 8c, g, d, h), except that of adults from sample set S which had very high mean and variance in the San Joaquin River box (Fig. 8g).

In situ mortality of nauplii and copepodites generally increased through time in the low-salinity box but not that of adults, and in situ mortality values in the San Joaquin (Figs. 8 and 9) and Sacramento (Fig. 8) boxes were similar to each other and did not vary systematically over time (sample set R; Table 3; Fig. 9). In situ mortality of nauplii and copepodites in the low-salinity box had extremely high values in 2007 owing

Fig. 8 In situ mortality (Eq. 4) of *Pseudodiaptomus forbesi* vs. salinity by life stage and region (symbols, see legend). **a, e** Nauplii. **b, f** Copepodites. **c, g** Adult males. **d, h** Adult females. **a–d** Sample set R. **e–h** Sample sets S and T (by region). Sample set S shown by star symbols with error bars indicating 95% CI; results for unsexed adults in **g**. Note that scales differ among rows
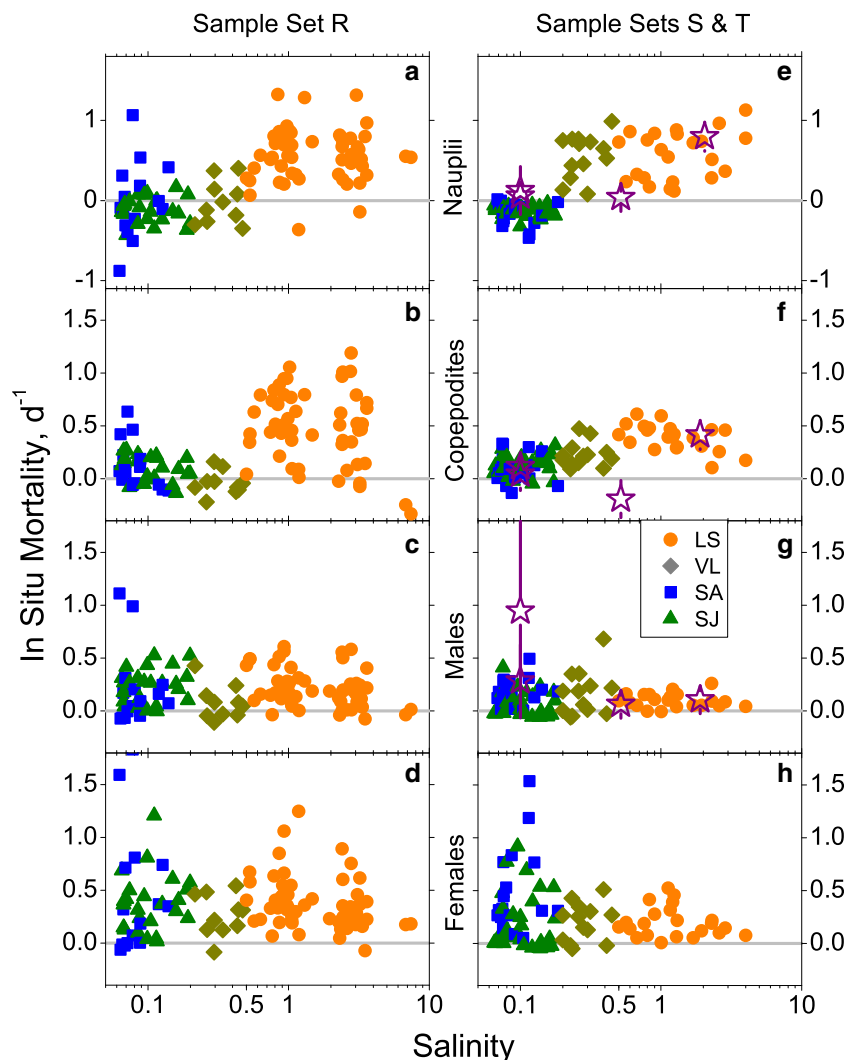
Fig. 9 In situ mortality rate of *Pseudodiaptomus forbesi* vs. year by life stage for two boxes: **a–d** low-salinity box; **e–h** San Joaquin River box. **a**, **e** Nauplii. **b**, **f** Copepodites. **c**, **g** Adult males. **d**, **h** Adult females. Sample sets R and T: crosses indicate single samples and circles indicate means of three or more samples with 95% CI. Sample set S shown by star symbols with error bars indicating 95% CI. Arrows indicate values of outliers

Discussion
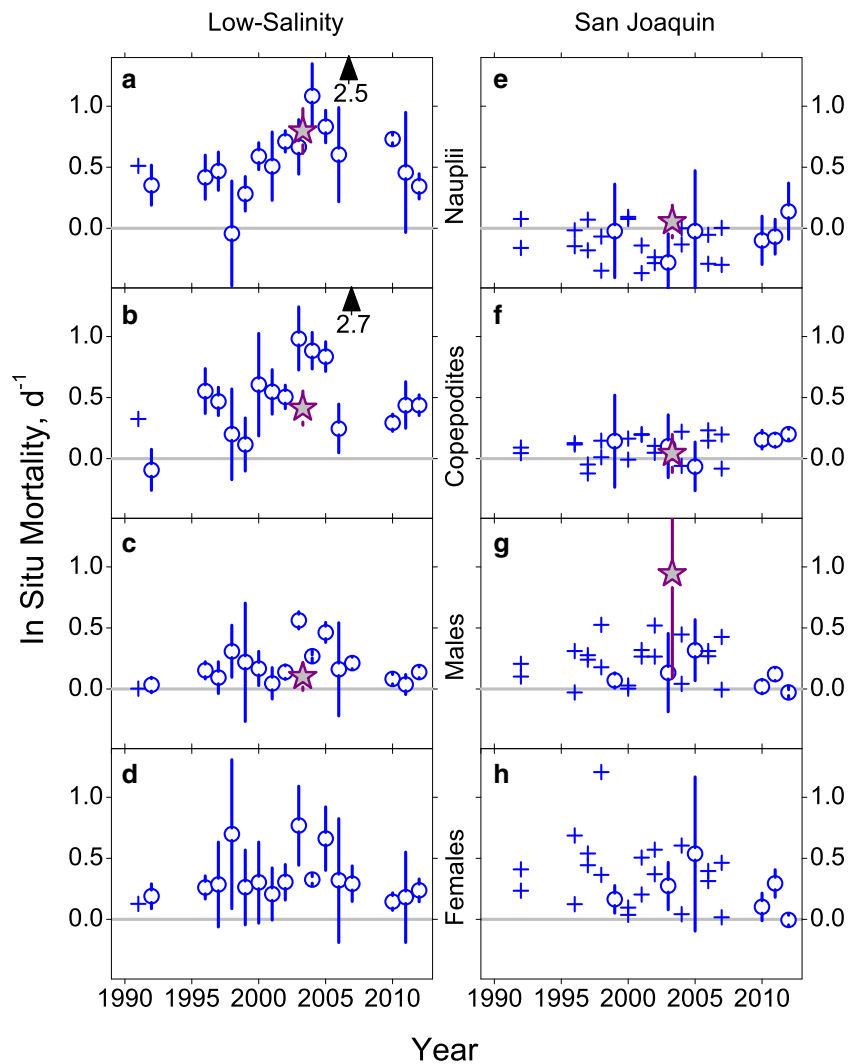
to the exceptionally high net rate of transport into that box (Fig. 7). Conversely, in 1998, in situ mortality of nauplii in the low-salinity box was low and uncertain (Fig. 9a). This was the highest flow year in the record (Fig. 4), when the entire population was shifted seaward (Fig. 5) and stratification was strong, so the relationship between salinity and abundance based on vertically integrated samples may be inaccurate.

Discussion

Estimates of in situ mortality are far more difficult to determine and therefore less frequent than estimates of reproduction or growth (Ohman and Wood 1995; Hirst and Kiørboe 2002). Ohman (2012) argued that the difficulties represent a challenge rather than an impediment and outlined some ways of confronting the challenge. These include careful design of the spatial and temporal densities of sampling, adequate replication, and good data on underlying development rates. Many samples taken at suitable time and space intervals can

average out effects of violations of some assumptions of the vertical-life-table method (Ohman 2012). High sampling density can also smooth out errors inherent in using count data and to some extent the errors due to uncertainty in the rate estimates (Kimmerer 2015).

None of these recommendations addresses violations of the assumption in the vertical-life-table method of a closed or spatially uniform population. We have done so here by incorporating explicit calculations of movement obtained from fine-scale numerical models into an analysis using coarse spatial boxes, which match our research focus on regional patterns of mortality, particularly in low-salinity water.

Our results demonstrate both the feasibility of estimating mortality of planktonic populations in dynamic estuaries and the effort required to do it. A few previous estimates of zooplankton mortality have been made in estuaries with limited circulation (Barlow 1955; Kimmerer and McKinnon 1987, 1990; Tiselius et al. 2008). Even in our study, it was possible only under benign conditions of low freshwater flow and relatively steady seasonal population abundance and using a

large number of samples. Nevertheless, the chief methodological lesson from our study is the need to account explicitly for water movement in estimating mortality of plankton in any estuary with strong tidal mixing and spatial gradients in abundance.

The adjustments for movement (Eqs. 1–4) have two implications. First, failure to account for spatial subsidies can result in substantial underestimates of actual mortality due to in situ processes (see Table A2 for nauplii and copepodites in the low-salinity box LS). Moreover, spatial subsidies exist when local in situ mortality exceeds what the local population can afford (Dam and Tang 2001). Second, failure to account for spatial losses results in incorrectly assigning these losses to in situ mortality, resulting in an overestimate. The resulting incorrect estimates of in situ mortality thereby obscure its stage-specific and temporal variation, which are essential for understanding population dynamics.

Assumptions of the Mortality Method

The principal assumptions underlying the vertical-life-table method applied here are that the age distribution is stable, immigration and emigration are either negligible or accounted for, and mortality is constant across one or more developmental stages (Ohman 2012; Gentleman et al. 2012). The assumption of a stable age distribution is unlikely to be met in a dynamic estuarine population. Violations of this assumption manifest as variability among samples taken in the same region at the same time (e.g., Fig. 9). This variability can be large, and its effect is overcome mainly through replication and repeated sampling under similar conditions, e.g., summer–fall during the peak in abundance of *P. forbesi*.

Mortality is often assumed to vary among life stages or to be constant between successive pairs of life stages (Mullin and Brooks 1970). However, the variability inherent in counts of stage frequencies and in estimates of life-stage durations make stage-specific estimates of mortality highly uncertain (Kimmerer 2015). Therefore, we assumed mortality to be constant across each major life stage, e.g., all copepodites.

Negative in situ mortality may seem anomalous and algorithms have been developed to prevent calculation of negative mortality rates (Wood 1994). Nevertheless, negative mortality is consistent with the equations for both apparent mortality of developing stages (Kimmerer 2015) and transport of all stages (Eq. 4). Given the high variability inherent in the use of count data and the uncertainty in stage durations (Kimmerer 2015), mortality rates estimated from single samples may easily be negative. Truncating or discarding negative values introduces bias in summary statistics and may obscure a problem in the underlying methods. Negative apparent mortality in individual samples can arise through sampling variability, so the mortality estimates are meaningful only when averaged over an adequate number of samples.

Apparent mortality estimates can also be biased, sometimes appearing as negative, if assumptions of the methods are not met. Apparent mortality of developing stages may be negative because early stages are under-sampled resulting in high relative abundance of later stages. Under-sampling of copepodite stage 1 in sample set R would have artificially depressed mortality of copepodites, so we corrected for this source of bias (Supplementary Information). Under-sampling of adults can result in overestimates of their mortality and negative estimates of mortality of nauplii because of an underestimate of population egg production, and this could not be corrected with the available data. Under-sampling of adults may explain the negative mean in situ mortality of nauplii in the San Joaquin box (Fig. 9e). Water is clearer there than in the other regions and may have caused adults and late copepodites to remain on the bottom by day where they were unavailable to the sampling gear (Kimmerer and Slaughter 2016), although we discarded data from one station where this effect was obvious. Apparent mortality of developing life stages can also be consistently negative if a spatial subsidy enhances abundance of later life stages.

In situ mortality is less likely to be negative than apparent mortality because the spatial subsidy is taken into account (e.g., copepodites in the low-salinity box in sample sets R and S; Table 3). However, in situ mortality could be negative for a given sample because of sampling variability, inadequate spatial coverage in samples used to estimate subsidies into a spatial box (Figs. 4 and 5), or violations of assumptions of the vertical-life-table method as discussed above.

The box model may not reflect the movements of copepods in some instances, such as in 1998 (Fig. 5). That year had the highest freshwater flow in the time period. The low-salinity box was centered in western Suisun Bay (Figs. 1 and 3), and for nearly half of the tidal cycle, the physical low-salinity zone was in Carquinez Strait (Fig. 1), where stratification is usually strong. The particle-tracking model accurately captures these conditions and therefore the exchange coefficients are accurate. However, copepod abundance was determined by oblique tows and there is no information on vertical distributions of copepods in the sampling data. For these conditions, depth-specific sampling coupled with an individual-based model on a particle-tracking framework may have been more suitable (Batchelder et al. 2002).

The Role of Hydrodynamics

Studies of the influence of estuarine exchange on plankton populations have a long history (Rogers 1940; Ketchum 1954; Barlow 1955). The general themes of the literature concern the minimum rate of growth of planktonic populations necessary to offset losses to sea and the ways that organisms can use depth- or time-varying estuarine circulation to recruit to, or be retained in, an estuary (Cronin and Forward 1979).

Organisms may overcome net seaward transport through, e.g., tidal vertical migration or selective tidal stream transport (Cronin and Forward 1979). Exchange with areas of high productivity can subsidize areas of low productivity (Lopez et al. 2006). In a model estuarine planktonic system, an optimum exchange rate maximized overall system productivity (Cloern 2007).

We accounted for the movement of copepods by the use of the Gross Exchange Matrix approach (Kremer et al. 2010) to represent exchange between boxes from a combination of advective transport driven by tidally averaged flows and mixing driven by estuarine circulation and tidal flows. The implicit assumption of well-mixed conditions within each box is known to lead to some inaccuracy relative to high-resolution hydrodynamic and transport models but is a suitable approach in simulations with high uncertainty in ecological parameters (Kremer et al. 2010). The particle-tracking model from which exchange was estimated included supportable assumptions about the role of tidal vertical migration in the larger life stages (Kimmerer et al. 2002). Nauplii were assumed to be too small to maintain the steady swimming speeds required for retention, at least 0.5 mm s^{-1} (Kimmerer et al. 2014).

Exchange among regions of the estuary represented by boxes in our model does three things: (1) It removes copepods from the model domain via diversions of freshwater from the Delta, mainly from the San Joaquin box, and via net losses to higher salinity in the low-salinity box, (2) it provides a spatial subsidy from areas of high to areas of low productivity, and (3) it greatly complicates the estimation of mortality. Exchange is mediated by both advection and dispersion. The influence of advection on exchange increases as freshwater flow increases, as can be seen in the increase in losses to seaward with increasing flow (lower X2; Fig. 6). Note, however, that gains are governed more by spatial gradients than exchange rates, which is why net gains to the low-salinity zone increase rather than decrease as freshwater flow decreases (Fig. 7 inset for X2).

The range of freshwater flows included in the analysis was constrained to values that occurred during the sampling periods, i.e., summer–autumn when abundance of *P. forbesi* is high and not changing rapidly (Kimmerer et al. 2017). Higher flows than are included in our model would have resulted in larger rates of loss from the low-salinity box to seaward, particularly for passive particles but also for particles with a fixed pattern of tidal vertical migration. However, actual vertical migration behaviors of copepods can be flexible (Verheye and Field 1992), and *P. forbesi* may respond to higher freshwater flow through a higher rate of tidal vertical migration which can offset the rate of loss (Kimmerer et al. 2014).

We used boxes whose boundaries are not fixed geographically but move with the salinity field. This is an uncommon practice but was selected for ease of interpretation. Species of estuarine plankton and nekton generally are distributed across a salinity range rather than a geographic range. That is, they live in a moving frame of reference and are most suitably analyzed in that frame, which can be readily tied to salinity (Laprise and Dodson 1993).

In the discussion below, we emphasize the low-salinity and San Joaquin boxes over the others for several reasons. As the terminal boxes in the model domain, these are subject to losses to seaward (low-salinity box) and to water diversions in the Delta (most in the San Joaquin box). The Sacramento and very low-salinity boxes had negligible (< 0.003 day^{-1}) losses from the model domain. The very low-salinity box was small and fewer samples were taken there, resulting in high variability in abundance and therefore in net gains and in situ mortality (Table 3). The Sacramento River box had large confidence limits for annual values of in situ mortality (Table 3) and subsidies (Fig. 6), possibly owing to the widely varying spatial extent of this box. Moreover, most of the freshwater flow into and through the Delta comes from the Sacramento River, and copepod abundance in some areas can be diluted under higher flows.

The low-salinity region is of particular interest because of the importance of *P. forbesi* to feeding by small planktivorous fishes there. Since many of these fishes appear to be food limited, the magnitude of mortality in and subsidies to the low-salinity region are critical factors determining abundance of food for these fishes.

The San Joaquin box is the population center where *P. forbesi* is most abundant and is therefore the principal source of subsidies to other regions. Diversion pumps in the south Delta and numerous smaller diversion pumps and siphons throughout the Delta remove large quantities of water and aquatic organisms from the system and have been a focus of ongoing controversy (Lund et al. 2007). Losses to these diversions from the San Joaquin box ranged from 0.04 to 0.07 day^{-1}, increasing with X2 as the spatial extent of the San Joaquin box was compressed further to the east (Figs. 1 and 5d, h). Since the San Joaquin box receives little subsidy from other boxes (Fig. 6l), this pumping probably imposes a substantial limit on growth rate of the entire population.

Patterns, Causes, and Consequences of Mortality in *Pseudodiaptomus forbesi*

The abundance patterns (Figs. 2 and 3) make clear that *P. forbesi* has been continuously abundant for two decades starting in 1990, though with a decrease in abundance over the first ~ 5 years of this record (Kayfetz and Kimmerer 2017). Interannual variation in mortality was mostly low over the entire 21-year period of the study and was confined largely to anomalously low in situ mortality values for nauplii and copepodites in 1998 (discussed above) and high net gains

during 2007 (Fig. 7). The 2007 values were a consequence of an anomalous spatial pattern of abundance (Fig. 5d), but we do not know its cause.

Spatial patterns were characterized by sharp gradients in abundance vs. salinity and an ontogenetic shift in peak abundance toward higher salinity (Fig. 3). Sharp gradients could result from high seaward in situ mortality rates or from a reduction in dispersion, which is possible through tidal vertical migration as shown for this copepod population in Kimmerer et al. (2014). Since adults are likely the most competent life stage at avoiding washout through tidal vertical migration, the steeper abundance gradients of developing stages (Fig. 3) are most likely a result of the high in situ mortality of nauplii and possibly copepodites at salinity above ~ 0.5 (Fig. 8).

Mortality patterns differed somewhat among the three sample sets (Table 3). This was a result of differences in temporal and spatial coverage, life stages sampled, and environmental conditions. Of the three sample sets, only set S was designed specifically to examine mortality rates of all life stages, and none were designed to account for movement between regions of the estuary. Thus, the differences arose essentially because the sampling programs did not provide sufficient spatial and temporal coverage for analysis of mortality at scales finer than those resolved here, i.e., within boxes and across years.

In situ mortality of adult females averaged about twice that of males. Female-biased sex ratios, which usually imply lower mortality of females than males, are often observed in field studies of planktonic copepods (Hirst et al. 2010). The elevated mortality in females in our study is likely due to size-selective predation by visually feeding planktivorous fish. Females are $\sim 17\%$ longer and $\sim 19\%$ wider and are more pigmented than males, and often carry egg sacs, rendering them more visible than males. More generally, predation by fish is often skewed toward higher consumption of female copepods than males (Hirst et al. 2010), while the opposite may be true for invertebrate predators. In the upper SFE, fish are the predominant predators on copepods since invertebrate predators are uncommon (e.g., mysids; Feyrer et al. 2003).

In situ mortality of nauplii was highest in the low-salinity box (Fig. 9; Table 3). The planktonic foodweb in this region during summer–autumn is strongly controlled by the invasive clam *Potamocorbula amurensis* (Alpine and Cloern 1992). Although *Corbicula fluminea* is abundant in fresh water of the Delta, its per-biomass grazing rate is lower than that of *P. amurensis*. Clam grazing suppresses phytoplankton biomass (Kimmerer and Thompson 2014) and abundance of microzooplankton (Greene et al. 2011). Copepods can have strong escape responses to clam siphons; nevertheless, during summer–autumn of 1988–2008, clams consumed ~ 0.20 day^{-1} of nauplii of the copepod *Eurytemora affinis* in the low-salinity zone (Kimmerer and Lougee 2015). *Pseudodiaptomus forbesi* nauplii have a similar escape response to that of *E. affinis* (Kimmerer and Lougee 2015), so this figure can be applied to *P. forbesi*. In addition, the predatory copepod *Acartiella sinensis* consumed *P. forbesi* nauplii at a rate of ~ 0.12 day^{-1} during July–October 1994–2012 (Slaughter et al. 2016). The total of ~ 0.32 day^{-1} for these two consumers alone is about half of total mortality of nauplii in the region (Table 3). These two sources of mortality are likely a significant control on abundance of *P. forbesi* in the low-salinity region and may be the cause of the contraction of the range of this copepod in ~ 1993 (Kayfetz and Kimmerer 2017), which is linked to the increase in subsidy to the low-salinity box (Fig. 7).

The ability of a closed population to withstand mortality depends on the population's capacity to reproduce and develop (Dam and Tang 2001). Egg production rate of *P. forbesi* averaged ~ 2 eggs female^{-1} day^{-1} over the duration of this study. At the mean development times and calculated in situ mortality rates for each life stage in the low-salinity box (Table 3), and assuming a 1:1 sex ratio, each generation would be $\sim 1\%$ as abundant as the previous. This rate of loss clearly can be sustained only with a spatial subsidy.

The mortality patterns of *P. forbesi* in the low-salinity box reflected those calculated for the small cyclopoid *Limnoithona tetraspina*, which is rather uniformly abundant at salinity ~ 1–10 (Kimmerer 2015). In that population, the median mortality rates in summer 2007 were 0.13 day^{-1} for nauplii, 0.05 day^{-1} for copepodites, and 0.03 day^{-1} for adults. The relative values of these rates are consistent with those for the same life stages of *P. forbesi* in the low-salinity spatial box (Fig. 9a–e). The lower absolute values for *L. tetraspina* reflect their small size and cryptic behavior which limit predation (Sullivan et al. 2016) and which are consistent with lower reproductive and development rates that limit their "affordable mortality" (Dam and Tang 2001).

A key consequence of the high mortality rate of nauplii and copepodites in the low-salinity zone is that abundance of the key prey of some of the fishes there is greatly depressed. This in turn has led to wholesale shifts in distributions of various fish species following the invasion by *Potamocorbula amurensis* (Nichols et al. 1990). Abundance of striped bass *Morone saxatilis* and longfin smelt *Spirinchus thaleichthys* declined soon after the clam invasion (Thomson et al. 2010; Mac Nally et al. 2010). At the same time, abundance of northern anchovy *Engraulis mordax* declined in the low-salinity region, presumably because anchovies abandoned this now unproductive area in favor of high-salinity waters that had remained productive (Kimmerer 2006). In addition, juvenile striped bass became less abundant in the channels and more abundant in shallow, nearshore areas, presumably because of better foraging opportunities (Sommer et al. 2011). Abundance of the endangered delta smelt *Hypomesus transpacificus* may have increased in the northern Delta even as it decreased in the low-salinity region, implying a shift

away from food-limited open brackish waters of the estuary (Sommer and Mejia 2013).

Spatial Subsidies and In-Situ Mortality

Spatial subsidies are a common feature of ecosystems, particularly marine and estuarine systems where rates of exchange can be high. Examples include outwelling of organic matter from marshes (Odum 1980), subsidies of nutrients and other materials to marine islands (Polis et al. 1997), consumption at the edges of habitats resulting in transfer of material from one habitat to another (Jumars 2007), larval fish recruitment (Cowen et al. 2006), and transport through active migrations either vertically (Longhurst et al. 1990) or laterally (Kneib 1997). The pelagic zones of estuaries can be subsidized by, e.g., nutrients from land (Nixon et al. 1986) or sea (Smith and Hollibaugh 1997), detrital matter that supports a microbial-based foodweb (Sobczak et al. 2005), or phytoplankton to support high benthic grazing (Kimmerer and Thompson 2014). Stable isotope studies across 14 estuaries in British Columbia revealed contrasting subsidies in both terrestrial and marine nitrogen to the foodwebs supporting clams (Harding et al. 2015). Patchy distributions of clams in the California Delta resulted in highly variable phytoplankton biomass and revealed the importance not only of mixing and advection but also the utility of a whole-system view of production and consumption (Lopez et al. 2006).

Our analysis and results demonstrate that in situ mortality and spatial subsidies of planktonic organisms are two sides of the same coin. That is, spatial subsidies can shore up a population in places where spatial losses and in situ mortality together exceed its productive capacity.

The low-salinity zone of the SFE is heavily subsidized in phytoplankton biomass, mainly from the Delta, because of high losses to grazing by clams (Kimmerer and Thompson 2014). Here we have shown that it is also heavily subsidized in *P. forbesi*, for similar reasons. This copepod comprised ~ 55% of the prey biomass of the declining and endangered delta smelt in that habitat during June–September of 2005–2006 (Slater and Baxter 2014). Declines in delta smelt have been attributed in part to poor feeding conditions in their key low-salinity habitat, particularly during summer (Slater and Baxter 2014; Hammock et al. 2015). The current low abundance of *P. forbesi* in the low-salinity zone is due to high mortality of early life stages and would be zero if not for the subsidy of copepods of all life stages from the freshwater Delta.

References

Aksnes, D.L., and M.D. Ohman. 1996. A vertical- life- table approach to zooplankton mortality estimation. *Limnology and Oceanography* 41: 1461–1469.

Alpine, A.E., and J.E. Cloern. 1992. Trophic interactions and direct physical effects control phytoplankton biomass and production in an estuary. *Limnology and Oceanography* 37: 946–955.

Barlow, J.P. 1955. Physical and biological processes determining the distribution of zooplankton in a tidal estuary. *Biological Bulletin* 109: 211–225.

Batchelder, H.P., C.A. Edwards, and T.M. Powell. 2002. Individual-based models of copepod populations in coastal upwelling regions: implications of physiologically and environmentally influenced diel vertical migration on demographic success and nearshore retention. *Progress in Oceanography* 53: 307–333.

Baxter, R., R. Breuer, L. Brown, L. Conrad, F. Feyrer, S. Fong, K. Gehrts, et al. 2010. *2010 Pelagic organism decline work plan and synthesis of results*. Sacramento: Interagency Ecological Program for the San Francisco Estuary.

Bryant, M.E., and J.D. Arnold. 2007. Diets of age-0 striped bass in the San Francisco Estuary, 1973–2002. *California Fish and Game* 93: 1–22.

Cloern, J.E. 2007. Habitat connectivity and ecosystem productivity: implications from a simple model. *American Naturalist* 169: E21–E33.

Cowen, R.K., C.B. Paris, and A. Srinivasan. 2006. Scaling of connectivity in marine populations. *Science* 311: 522–527.

Cronin, T.W., and R.B. Forward Jr. 1979. Tidal vertical migration: an endogenous rhythm in estuarine crab larvae. *Science* 205: 1020–1022.

Dam, H.G., and K.W. Tang. 2001. Affordable egg mortality: constraining copepod egg mortality with life history traits. *Journal of Plankton Research* 23: 633–640.

Drinkwater, K.F., and K.T. Frank. 1994. Effects of river regulation and diversion on marine fish and invertebrates. *Aquatic Conservation: Marine and Freshwater Ecosystems* 4: 135–151.

Durand, J.R. 2010. Determinants of seasonal abundance in key zooplankton of the San Francisco Estuary. Master's thesis, San Francisco State University, San Francisco, CA.

Eiane, K., D.L. Aksnes, M.D. Ohman, S. Wood, and M.B. Martinussen. 2002. Stage-specific mortality of *Calanus* spp. under different predation regimes. *Limnology and Oceanography* 47: 636–645.

Feyrer, F., B. Herbold, S.A. Matern, and P.B. Moyle. 2003. Dietary shifts in a stressed fish assemblage: consequences of a bivalve invasion in the San Francisco Estuary. *Environmental Biology of Fishes* 67: 277–288.

Genin, A., L. Haury, and P. Greenblatt. 1988. Interactions of migrating zooplankton with shallow topography: predation by rockfishes and intensification of patchiness. *Deep-Sea Research Part II* 35: 151–175.

Gentleman, W.C., P. Pepin, and S. Doucette. 2012. Estimating mortality: clarifying assumptions and sources of uncertainty in vertical methods. *Journal of Marine Systems* 105: 1–19.

Greene, V.E., L.J. Sullivan, J.K. Thompson, and W.J. Kimmerer. 2011. Grazing impact of the invasive clam *Corbula amurensis* on the microplankton assemblage of the northern San Francisco Estuary. *Marine Ecology Progress Series* 431: 183–193.

Gross, E.S., M.S. MacWilliams, C.D. Holleman, and T.A. Hervier. 2010. POD 3–D particle tracking modeling study. Particle tracking model testing and applications report. Report to the Interagency Ecological Program. Available from: http://www.science.calwater.ca.gov/pdf/workshops/POD/GrossEtAl_POD3D_Particle_tracking_2010.pdf. Accessed 26 April 2018.

Hammock, B.G., J.A. Hobbs, S.B. Slater, S. Acuna, and S.J. Teh. 2015. Contaminant and food limitation stress in an endangered estuarine fish. *Science of the Total Environment* 532: 316–326.

Harding, J.M.S., M.R. Segal, and J.D. Reynolds. 2015. Location is everything: evaluating the effects of terrestrial and marine resource subsidies on an estuarine bivalve. *PLoS One* 10.

Hirst, A.G., and A.J. Bunker. 2003. Growth of marine planktonic copepods: global rates and patterns in relation to chlorophyll a, temperature, and body weight. *Limnology and Oceanography* 48: 1988–2010.

Hirst, A.G., and T. Kiørboe. 2002. Mortality of marine planktonic copepods: global rates and patterns. *Marine Ecology Progress Series* 230: 195–209.

Hirst, A.G., D. Bonnet, D.V.P. Conway, and T. Kiørboe. 2010. Does predation control adult sex ratios and longevities in marine pelagic copepods? *Limnology and Oceanography* 55: 2193–2206.

Hook, S.E., and N.S. Fisher. 2001. Reproductive toxicity of metals in calanoid copepods. *Marine Biology* 138: 1131–1140.

Jassby, A.D., W.J. Kimmerer, S.G. Monismith, C. Armor, J.E. Cloern, T.M. Powell, J.R. Schubel, and T.J. Vendlinski. 1995. Isohaline position as a habitat indicator for estuarine populations. *Ecological Applications* 5: 272–289.

Johnson, J.K. 1980. Effects of temperature and salinity on production and hatching of dormant eggs of *Acartia californiensis* (Copepoda) in an Oregon estuary. *Fishery Bulletin* 77: 567–581.

Jumars, P.A. 2007. Habitat coupling by mid-latitude, subtidal, marine mysids: import-subsidised omnivores. *Oceanography and Marine Biology: An Annual Review* 45: 89–138.

Kayfetz, K., and W. Kimmerer. 2017. Abiotic and biotic controls on the copepod *Pseudodiaptomus forbesi* in the upper San Francisco Estuary. *Marine Ecology Progress Series* 581: 85–101.

Ketchum, B.H. 1954. Relation between circulation and planktonic populations in estuaries. *Ecology* 35: 191–200.

Kimmerer, W.J. 2006. Response of anchovies dampens effects of the invasive bivalve *Corbula amurensis* on the San Francisco Estuary foodweb. *Marine Ecology Progress Series* 324: 207–218.

Kimmerer, W.J. 2015. Mortality estimates of stage-structured populations must include uncertainty in stage duration and relative abundance. *Journal of Plankton Research* 37: 939–952.

Kimmerer, W.J., and L.A. Lougee. 2015. Bivalve grazing causes substantial mortality to an estuarine copepod population. *Journal of Experimental Marine Biology and Ecology* 473: 53–63.

Kimmerer, W.J., and A.D. McKinnon. 1987. Growth, mortality, and secondary production of the copepod *Acartia tranteri* in Westernport Bay, Australia. *Limnology and Oceanography* 32: 14–28.

Kimmerer, W.J., and A.D. McKinnon. 1990. High mortality in a copepod population caused by a parasitic dinoflagellate. *Marine Biology* 107: 449–452.

Kimmerer, W.J., and K.A. Rose. 2018. Individual-based modeling of delta smelt population dynamics in the upper San Francisco Estuary III. Effects of entrainment mortality and changes in prey. *Transactions of the American Fisheries Society* 147: 223–243.

Kimmerer, W., and A. Slaughter. 2016. Fine-scale distributions of zooplankton in the northern San Francisco Estuary. *San Francisco Estuary and Watershed Science* 14 (3) Article 2). https://doi.org/10.15447/sfews.2016v14iss3art2.

Kimmerer, W.J., and J.K. Thompson. 2014. Phytoplankton growth balanced by clam and zooplankton grazing and net transport into the low-salinity zone of the San Francisco Estuary. *Estuaries and Coasts* 37: 1202–1218.

Kimmerer, W.J., W.A. Bennett, and J.R. Burau. 2002. Persistence of tidally-oriented vertical migration by zooplankton in a temperate estuary. *Estuaries* 25: 359–371.

Kimmerer, W.J., M.L. MacWilliams, and E.S. Gross. 2013. Variation of fish habitat and extent of the low-salinity zone with freshwater flow in the San Francisco Estuary. *San Francisco Estuary and Watershed Science*.

Kimmerer, W.J., E.S. Gross, and M.L. MacWilliams. 2014. Tidal migration and retention of estuarine zooplankton investigated using a particle-tracking model. *Limnology and Oceanography* 59: 901–906.

Kimmerer, W.J., T.R. Ignoffo, K.R. Kayfetz, and A.M. Slaughter. 2017. Effects of freshwater flow and phytoplankton biomass on growth, reproduction, and spatial subsidies of the estuarine copepod *Pseudodiaptomus forbesi*. *Hydrobiologia* 807: 113–130.

Kneib, R.T. 1997. The role of tidal marshes in the ecology of estuarine nekton. *Oceanography and Marine Biology Annual Review* 35: 163–220.

Koslow, J.A. 1981. Feeding selectivity of schools of northern anchovy, *Engraulis mordax*, in the Southern California Bight. *Fishery Bulletin* 79: 131–142.

Kremer, J.N., J.M.P. Vaudrey, D.S. Ullman, D.L. Bergondo, N. LaSota, C. Kincaid, D.L. Codiga, and M.J. Brush. 2010. Simulating property exchange in estuarine ecosystem models at ecologically appropriate scales. *Ecological Modelling* 221: 1080–1088.

LaBolle, E.M., J. Quastel, G.E. Fogg, and J. Gravner. 2000. Diffusion processes in composite porous media and their numerical integration by random walks: generalized stochastic differential equations with discontinuous coefficients. *Water Resources Research* 36: 651–662.

Laprise, R., and J.J. Dodson. 1993. Nature of environmental variability experienced by benthic and pelagic animals in the St. Lawrence Estuary, Canada. *Marine Ecology Progress Series* 94: 129–139.

Longhurst, A.R., A.W. Bedo, W.G. Harrison, E.J.H. Head, and D.D. Sameoto. 1990. Vertical flux of respiratory carbon by oceanic diel migrant biota. *Deep-Sea Research Part II* 37: 685–694.

Lopez, C.B., J.E. Cloern, T.S. Schraga, A.J. Little, L.V. Lucas, J.K. Thompson, and J.R. Burau. 2006. Ecological values of shallow-water habitats: implications for the restoration of disturbed ecosystems. *Ecosystems* 9: 422–440.

Lund, J., E. Hanak, W. Fleenor, R. Howitt, J. Mount, and P. Moyle. 2007. *Envisioning futures for the Sacramento-San Joaquin Delta*. San Francisco: Public Policy Institute of California, San Francisco.

Mac Nally, R., J. Thomson, W. Kimmerer, F. Feyrer, K. Newman, A. Sih, W. Bennett, et al. 2010. An analysis of pelagic species decline in the upper San Francisco Estuary using Multivariate Autoregressive modelling (MAR). *Ecological Applications* 20: 1417–1430.

MacIsaac, H.J., W.G. Sprules, and J.H. Leach. 1991. Ingestion of small-bodied zooplankton by zebra mussels (*Dreissena polymorpha*)—can cannibalism on larvae influence population dynamics? *Canadian Journal of Fisheries and Aquatic Sciences* 48: 2051–2060.

MacWilliams, M.L., and E.S. Gross. 2013. Hydrodynamic simulation of circulation and residence time in Clifton Court Forebay. *San Francisco Estuary and Watershed Science*. http://www.escholarship.org/uc/item/4q82g2bz.

MacWilliams, M.L., A.J. Bever, E.S. Gross, G.S. Ketefian, and W.J. Kimmerer. 2015. Three-dimensional modeling of hydrodynamics and salinity in the San Francisco Estuary: an evaluation of model accuracy, X2, and the low-salinity zone. *San Francisco Estuary and Watershed Science*. https://doi.org/10.15447/sfews.2015v13iss1art2.

Meyer, M., A. Barr, H. Lee, and M. Desbrun. 2002. Generalized barycentric coordinates on irregular polygons. *Journal of Graphics Tools* 7: 13–22.

Miller, C.B., J.K. Johnson, and D.R. Heinle. 1977. Growth rules in the marine copepod genus *Acartia*. *Limnology and Oceanography* 22: 326–335.

Monismith, S.G., W.J. Kimmerer, J.R. Burau, and M.T. Stacey. 2002. Structure and flow-induced variability of the subtidal salinity field in northern San Francisco Bay. *Journal of Physical Oceanography* 32: 3003–3019.

Mullin, M.M., and E.R. Brooks. 1970. Production of the planktonic copepod, *Calanus helgolandicus*. *Bulletin of the Scripps Institution Oceanography* 17: 89–103.

Nichols, F.H., J.K. Thompson, and L.E. Schemel. 1990. Remarkable invasion of San Francisco Bay (California, USA) by the Asian clam *Potamocorbula amurensis* .2. Displacement of a former community. *Marine Ecology Progress Series* 66: 95–101.

Nixon, S.W., C.A. Oviatt, J. Frithsen, and B. Sullivan. 1986. Nutrients and the productivity of estuarine and coastal marine systems. *Journal of the Limnological Society of South Africa* 12: 43–71.

Odum, E.P. 1980. The status of three ecosystem-level hypotheses regarding salt marsh estuaries: tidal subsidy, outwelling and detritus-based food chains. In *Estuarine perspectives*, ed. V.S. Kennedy, 485–495. Academic Press.

Ohman, M.D. 2012. Estimation of mortality for stage-structured zooplankton populations: what is to be done? *Journal of Marine Systems* 93: 4–10.

Ohman, M.D., and S.N. Wood. 1995. The inevitability of mortality. *ICES Journal of Marine Science* 52: 517–522.

Orsi, J., and W. Mecum. 1986. Zooplankton distribution and abundance in the Sacramento-san Joaquin Delta in relation to certain environmental factors. *Estuaries* 9: 326–339.

Orsi, J.J., and T.C. Walter. 1991. *Pseudodiaptomus forbesi* and *P. marinus* (Copepoda: Calanoida), the latest copepod immigrants to California's Sacramento-San Joaquin Estuary. In *Proceedings of the Fourth International Conference on Copepoda*, ed. S.-I. Uye, S. Nishida, and J.-S. Ho, 553–562. Hiroshima.

Polis, G.A., W.B. Anderson, and R.D. Holt. 1997. Toward an integration of landscape and food web ecology: the dynamics of spatially subsidized food webs. *Annual Review of Ecology and Systematics* 28: 289–316.

R Development Core Team. 2015. *R: a language and environment for statistical computing*. Vienna: R Foundation for Statistical Computing. doi.

Rogers, H. 1940. Occurrence and retention of plankton within an estuary. *Journal of the Fisheries Research Board of Canada* 5: 164–171.

Schmitt, F.G., D. Devreker, G. Dur, and S. Souissi. 2011. Direct evidence of tidally oriented behavior of the copepod *Eurytemora affinis* in the Seine estuary. *Ecological Research* 26: 773–780.

Slater, S.B., and R.D. Baxter. 2014. Diet, prey selection, and body condition of age-0 delta smelt, Hypomesus transpacificus, in the upper San Francisco Estuary. *San Francisco Estuary and Watershed Science*. https://doi.org/10.15447/sfews.2014v12iss3art1.

Slaughter, A.M., T.R. Ignoffo, and W. Kimmerer. 2016. Predation impact of *Acartiella sinensis*, an introduced predatory copepod in the San Francisco Estuary, USA. *Marine Ecology Progress Series* 547: 47–60.

Smith, S.V., and J.T. Hollibaugh. 1997. Annual cycle and interannual variability of ecosystem metabolism in a temperate climate embayment. *Ecological Monographs* 67: 509–533.

Sobczak, W.V., J.E. Cloern, A.D. Jassby, B.E. Cole, T.S. Schraga, and A. Arnsberg. 2005. Detritus fuels ecosystem metabolism but not metazoan food webs in San Francisco Estuary's freshwater Delta. *Estuaries* 28: 124–137.

Sommer, T., and F. Mejia. 2013. A place to call home: a synthesis of delta smelt habitat in the upper San Francisco Estuary. *San Francisco Estuary and Watershed Science*.

Sommer, T., C. Armor, R. Baxter, R. Breuer, L. Brown, M. Chotkowski, S. Culberson, et al. 2007. The collapse of pelagic fishes in the upper San Francisco Estuary. *Fisheries* 32: 270–277.

Sommer, T., F. Mejia, K. Hieb, R. Baxter, E. Loboschefsky, and F. Loge. 2011. Long-term shifts in the lateral distribution of age-0 striped bass in the San Francisco Estuary. *Transactions of the American Fisheries Society* 140: 1451–1459.

Sullivan, L.J., and W.J. Kimmerer. 2013. Egg development times of *Eurytemora affinis* and *Pseudodiaptomus forbesi* (Copepoda, Calanoida) from the upper San Francisco Estuary with notes on methods. *Journal of Plankton Research* 35: 1331–1338.

Sullivan, L.J., T.R. Ignoffo, B. Baskerville-Bridges, D.J. Ostrach, and W.J. Kimmerer. 2016. Prey selection of larval and juvenile planktivorous fish: impacts of introduced prey. *Environmental Biology of Fishes* 99: 633–646.

Tang, K.W., C.S. Freund, and C.L. Schweitzer. 2006. Occurrence of copepod carcasses in the lower Chesapeake Bay and their decomposition by ambient microbes. *Estuarine, Coastal and Shelf Science* 68: 499–508.

Thomson, J., W. Kimmerer, L. Brown, K. Newman, R. Mac Nally, W. Bennett, F. Feyrer, and E. Fleishman. 2010. Bayesian change-point analysis of abundance trends for pelagic fishes in the upper San Francisco Estuary. *Ecological Applications* 20: 1431–1448.

Tiselius, P., C.M.A. Borg, B.W. Hansen, P.J. Hansen, T.G. Nielsen, and B. Vismann. 2008. High reproduction, but low biomass: mortality estimates of the copepod *Acartia tonsa* in a hyper-eutrophic estuary. *Aquatic Biology* 2: 93–103.

UNESCO. 1981. *The practical salinity scale 1978 and the International Equation of State of seawater 1980*, Tenth report of the Joint Panel on Oceanographic Tables and Standards. Sidney: UNESCO.

Verheye, H.M., and J.G. Field. 1992. Vertical distribution and diel vertical migration of Calanoides carinatus (Krøyer, 1849) developmental stages in the southern Benguela upwelling region. *Journal of Experimental Marine Biology and Ecology* 158: 123–140.

Walter, T.C. 1989. Review of the new-world species of *Pseudodiaptomus* (Copepoda, Calanoida), with a key to the species. *Bulletin of Marine Science* 45: 590–628.

Wang, B., G. Zhao, and O.B. Fringer. 2011. Reconstruction of vector fields for semi-Lagrangian advection on unstructured, staggered grids. *Ocean Modelling* 40: 52–71.

Wood, S.N. 1994. Obtaining birth and mortality patterns from structured population trajectories. *Ecological Monographs* 64: 23–44.